Electronic Supplementary Material (ESI) for Environmental Science: Nano.

Detecting residual chemical disinfectant using an atomic Co-N_x-C anchored neuronal-like carbon catalyst modified amperometric sensor

Zehui Li, Guangya Jiang, Yaling Wang, Meijuan Tan, Youpeng Cao, EnzeTian, Lingling Zhang, Xiao Chen, Mengze Zhao, Yuheng Jiang, Yuyang Luo, Yuanhao Zheng, Zizhen Ma, Dongbin Wang, Wangyang Fu, Kaihui Liu, Cheng Tang, Jingkun Jiang

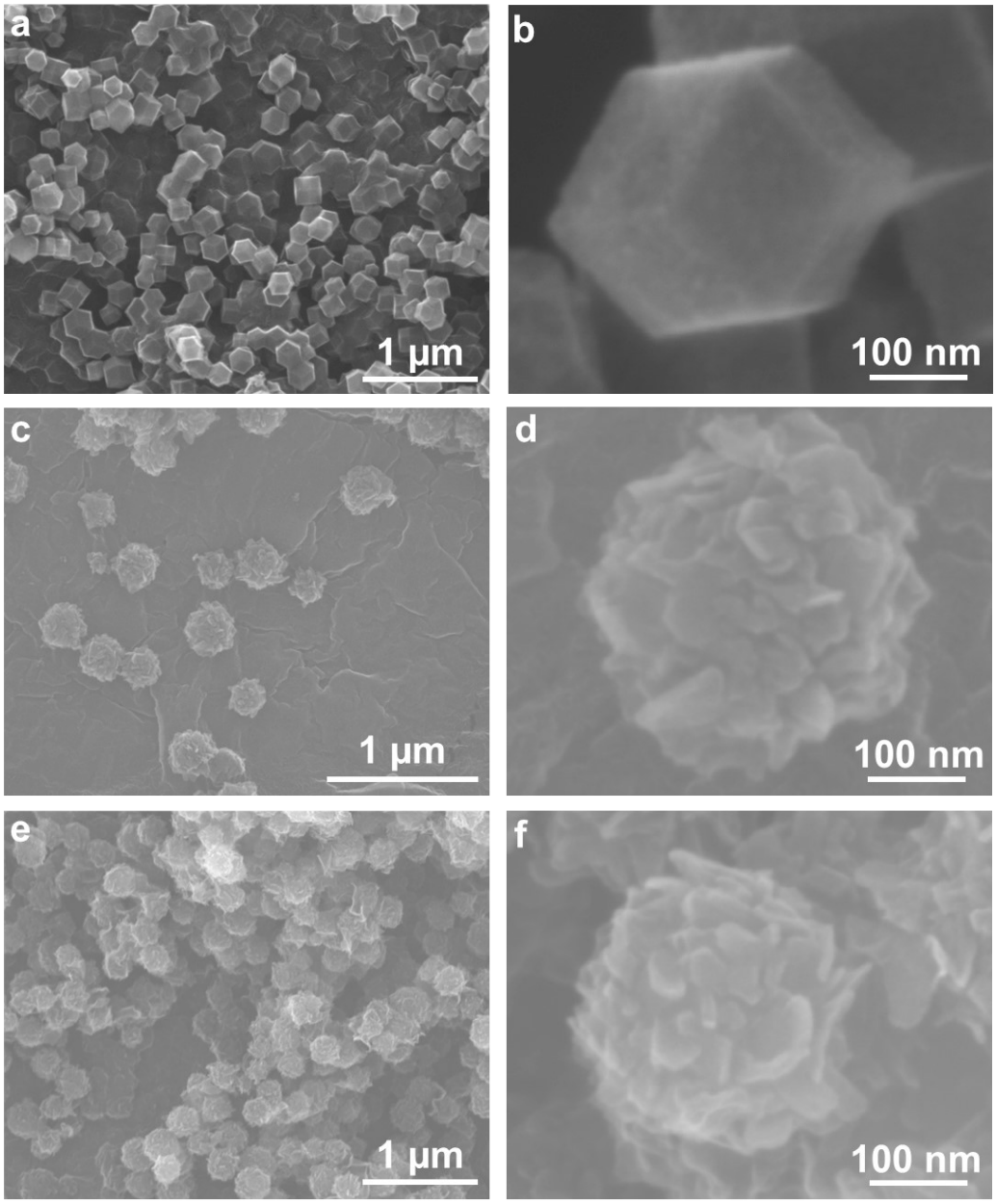

Figure S1. SEM images of aggregated (a,b) N/C, (c,d) CoSA-N/C, (e,f) CoSA-N/C@rGO with different magnification.

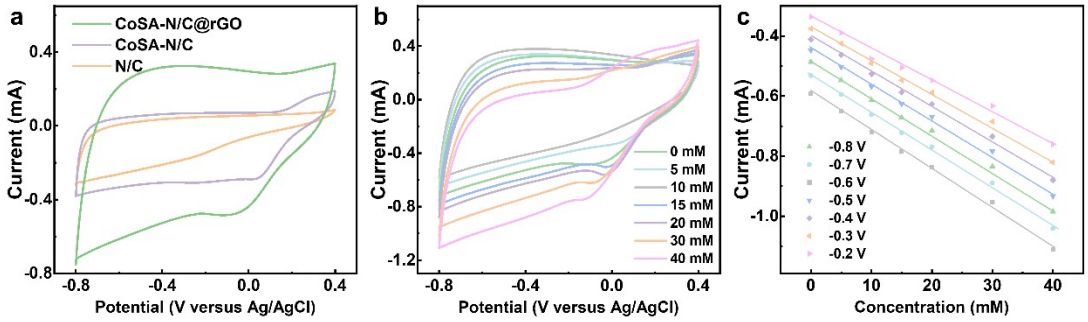

Figure S2. CV curves in PB electrolyte solutions (pH=7) with (a) different materials CoSA-N/C@rGO, CoSA-N/C, and N/C at 10 mM; (b) different concentration from 5 mM to 40 mM via CoSA-N/C@rGO and (c) its calibration curve of the amperometric response to the concentration at different potentials.

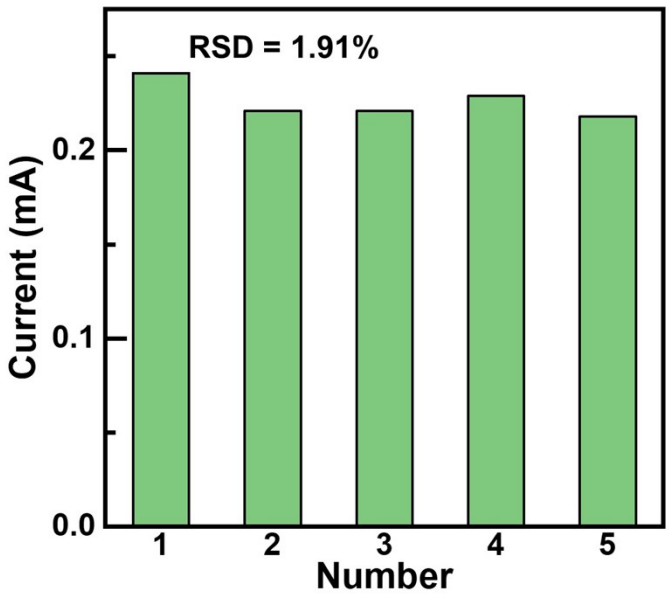

Figure S3. Current responses of five Co-N/C@G modified GCE sensors to 5 mM H_2O_2 at -0.7 V.

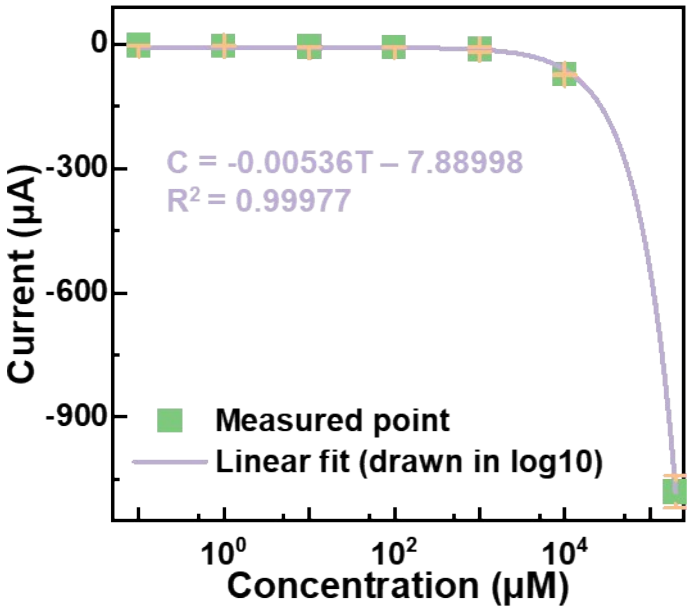

Figure S4. Calibration plot of steady-state current of response of the sensor to a range of liquid H_2O_2 from 100 nM to 1 mM .

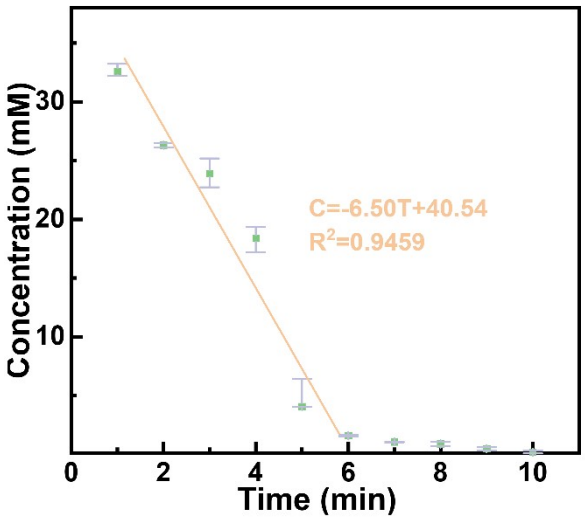

Figure S5. Change of residual H_2O_2 concentration on medical gloves with time.

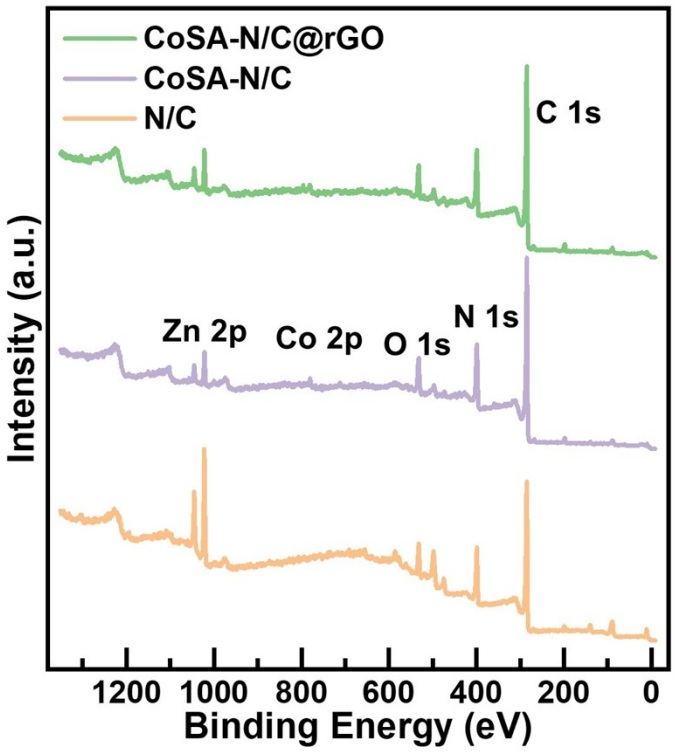

Figure S6. XPS survey spectra of CoSA-N/C@rGO, CoSA-N/C and N/C.

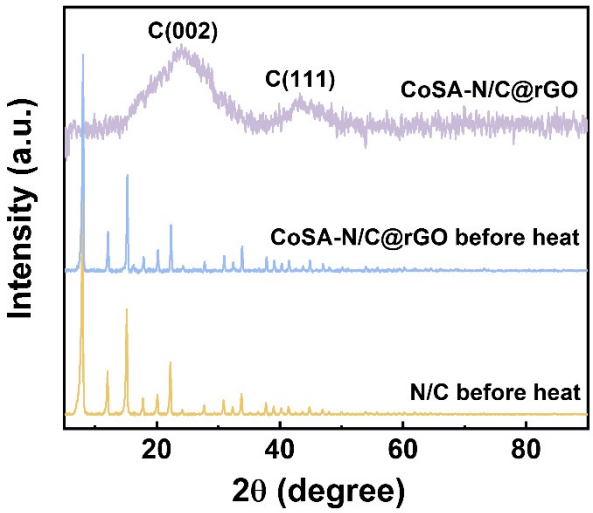

Figure S7. XRD pattern of CoSA-N/C@rGO catalyst, N/C and CoSA-N/C@rGO catalyst before pyrolysis.

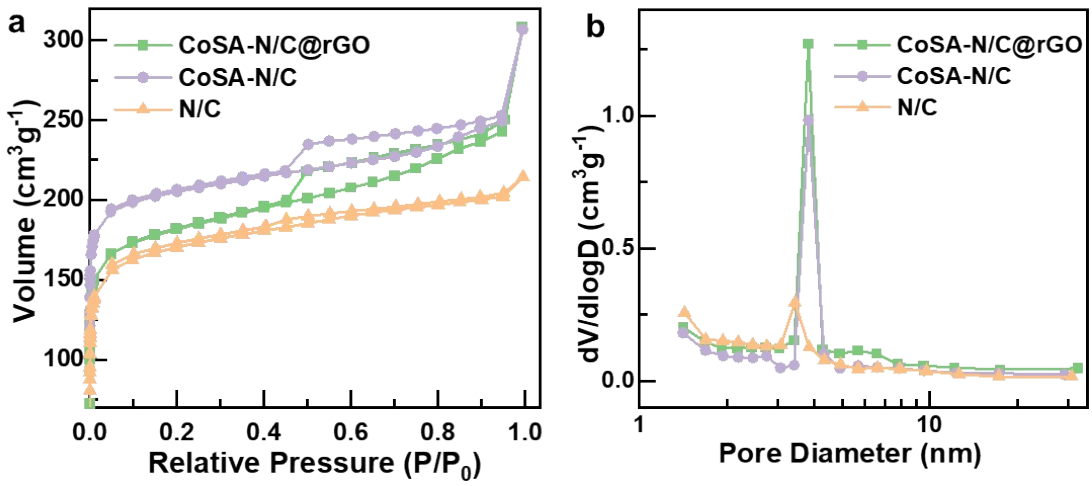

Figure S8. (a) Nitrogen adsorption-desorption isotherms and (b) the pore size distribution of N/C, CoSA-N/C, and CoSA-N/C@rGO.

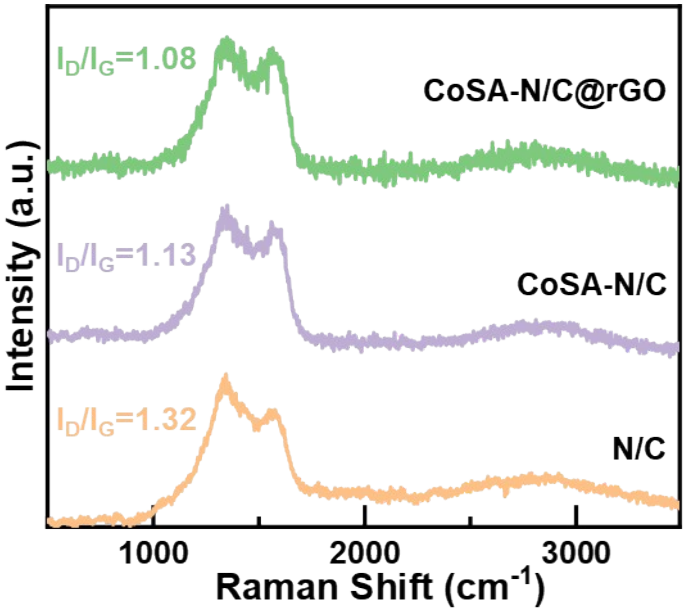

Figure S9. The Raman spectra of CoSA-N/C@rGO, CoSA-N/C, and N/C.

Table S1. Comparison of H_2O_2 sensors reported in recent studies.

Electrode materials	Sensitivity ($\mu A\ mM^{-1}\ cm^{-2}$)	Detection limit (μM)	Linear range (mM)	References
CoSA-N/C@G	**743.3** **599.2**	**0.25**	**0.00025 ~ 2.5** **5 ~ 50**	**This work**
Co-N/CNT	568.47	0.0324	0.00005 ~ 2.5 5 ~ 50	*Small, 2020, 16, 1902860.*
NC@rGO	272	3.322	0.005 ~ 20	*Microchim. Acta, 2018, 185, 501.*
Fe-NDs	None	0.3	0.001 ~ 0.6	*Front. Bioeng. Biotechnol., 2022, 9, 790849.*
3D Cu_2O-GA	None	0.37	0.001 ~ 1.47	*Anal. Chem., 2018, 90, 1983.*
2D Cu_2O-rGO-P	None	3.78	0.005 ~ 10.56	*Anal. Chem., 2018, 90, 1983.*
Co-MOF	83.1	3.76	0.005 ~ 9.0	*Sensor. Actuat. B, 2015, 215, 489.*
3D N-Co-CNT@NG	28.66	2	0.0020 ~ 7.449	*Biosens. Bioelectron., 2017, 89, 970.*
Fe_3C/NG	133.5	35	0.050 ~ 15	*Science Bulletin, 2015, 60, 522.*
Cu-CoTCPP	168	0.24	0.0005 ~ 18	*J. Mater. Chem. B, 2015, 3, 9340.*
NanoCoPc-Gr	185.7	14.6	0.0167 ~ 1.6	*Sensor. Actuat. B, 2015, 216, 298-306.*
Co_3O_4@rGO	None	100	0.0005 ~ 17.5	*Sci. Rep., 2017, 7, 43638.*
AuPd@G	186.86	1	0.005 ~ 11.5	*Biosens. Bioelectron., 2016, 85, 669.*
1% Mn-N/C	205.7	0.036	0.0001 ~ 50	*Environ. Sci.: Nano, 2018, 5, 1834.*
Fe/NOMC	709.63	5	0.008 ~ 23	*J. Electrochem. Soc., 2018, 165, H348.*

Table S2. Detection of H_2O_2 in real samples by Co-N/C@rGO sensor.

Samples	Prepared concentration of H_2O_2 (mM)	Detected value of H_2O_2 (mM)	RSD (n=3)	Recovery (%)
Tap water	0.05	0.0503	4.30%	100.70
Tap water	0.10	0.0982	2.21%	98.19

Table S3. XPS survey of element composition of CoSA-N/C@rGO.

	Species	N/C	CoSA-N/C	CoSA-N/C@rGO
Elemental composition (at%)	C 1s	69.68	72.63	72.72
	N 1s	17.78	18.34	18.66
	O 1s	7.09	6.88	6.30
	Co 2p	-	0.78	0.78
	Zn 2p	4.70	1.38	1.54
C (at%)	C-C/C=C	46.65	46.76	45.03
	C-O-C	2.24	3.07	3.82
	C=O	6.99	8.18	9.22
	C-N	13.79	14.62	14.66
N (at%)	Pyridinic N	11.29	7.51	9.78
	Co-Nx	-	2.43	2.19
	Pyrrolic N	5.18	5.11	4.70
	Quaternary N	1.05	2.07	1.48
	Oxidized N	0.27	0.77	0.46
	Chemisorbed N	0.00	0.46	0.05
Co (at%)	Co $2p_{3/2}$	-	0.34	0.40
	Co $2p_{3/2}$, sat.	-	0.08	0.06
	Co $2p_{1/2}$	-	0.17	0.21
	Co $2p_{1/2}$, sat.	-	0.19	0.11

Table S4. The comparison of porosity parameters of the catalysts.

Materials	Porosity parameter				
	S_{BET}[a] (m^2g^{-1})	V_t[b] (cm^3g^{-1})	V_{mic} (cm^3g^{-1})	V_{mic}/V_t (%)	Average pore size (nm)
N/C	623	0.33	0.23	69.84	2.13
CoSA-N/C	790	0.47	0.29	61.09	2.41
CoSA-N/C@rGO	670	0.48	0.24	49.87	2.85